Nonlinearity

PAPER • OPEN ACCESS

Travelling wave solutions of the cubic nonlocal Fisher-KPP equation: I. General theory and the near local limit

To cite this article: J Billingham and D J Needham 2022 *Nonlinearity* **35** 6098

OPEN ACCESS
IOP Publishing | London Mathematical Society Nonlinearity

Nonlinearity **35** (2022) 6098–6123 https://doi.org/10.1088/1361-6544/ac98ea

Travelling wave solutions of the cubic nonlocal Fisher-KPP equation: I. General theory and the near local limit

J Billingham[1,*] and D J Needham[2]

[1] School of Mathematical Sciences, The University of Nottingham, University Park, Nottingham NG7 2RD, United Kingdom
[2] School of Mathematics, The University of Birmingham, Edgbaston, Birmingham B15 2TT, United Kingdom

E-mail: John.Billingham@Nottingham.ac.uk

Received 21 March 2022, revised 12 August 2022
Accepted for publication 10 October 2022
Published 26 October 2022

Abstract

We study non-negative travelling wave solutions, $u \equiv U(x - ct)$ with constant wavespeed $c > 0$, of the cubic nonlocal Fisher-KPP equation in one spatial dimension, namely, $\frac{\partial u}{\partial t} = \frac{\partial^2 u}{\partial x^2} + u^2\left\{1 - \frac{1}{\lambda}\int_{-\infty}^{\infty}\phi\left(\frac{y-x}{\lambda}\right)u(y,t)\mathrm{d}y\right\}$, for $(x,t) \in \mathbb{R} \times \mathbb{R}^+$, where $u(x,t)$ is the population density. Here $\phi(y)$ is a prescribed, piecewise continuous, symmetric, nonnegative and nontrivial, integrable kernel, which is nonincreasing for $y > 0$, has a finite derivative as $y \to 0^+$ and is normalised so that $\int_{-\infty}^{\infty}\phi(y)\mathrm{d}y = 1$. The parameter λ is the ratio of the lengthscale of the kernel to the diffusion lengthscale. The quadratic version of the equation, with reaction term $u(1 - \phi^* u)$, has a unique travelling wave solution (up to translation) for all $c \geqslant c_{\min} = 2$. This minimum wavespeed is determined locally in the region where $u \ll 1$, (Berestycki *et al* 2009 *Nonlinearity* **22** 2813–44). For the cubic equation, we find that a minimum wavespeed also exists, but that the numerical value of the minimum wavespeed is determined globally, just as it is for the local version of the equation, (Billingham and Needham 1991 *Dynam. Stabil. Syst.* **6** 33–49). We also consider the asymptotic solution in the limit of a spatially-localised kernel, $\lambda \ll 1$, for which the travelling wave solutions are close to those of the cubic Fisher-KPP equation, $u_t = u_{xx} + u^2(1 - u)$. We find that when $\phi = o(y^{-3})$ as $y \to \infty$, the minimum

*Author to whom any correspondence should be addressed.
Recommended by Professor Arik Yochelis.

wavespeed is $\frac{1}{\sqrt{2}} + O(\lambda^4)$, but that when $\phi = O(y^{-n})$ with $1 < n \leqslant 3$, the minimum wavespeed is $\frac{1}{\sqrt{2}} + O(\lambda^{2(n-1)})$. In each case we determine the correction terms. We also compare these asymptotic solutions to numerical solutions and find excellent agreement for some specific choices of kernel.

Keywords: nonlocal reaction diffusion equation, travelling wave solution, asymptotic solution

Mathematics Subject Classification numbers: 35K57, 35B40, 35G20, 35C07, 65M06.

(Some figures may appear in colour only in the online journal)

1. Introduction

Nonlocal reaction–diffusion equations arise in many different scientific areas (see, for example, [3, 4]). The most studied of these is the nonlocal Fisher-KPP equation (NLFKPP)

$$\frac{\partial u}{\partial t} = \frac{\partial^2 u}{\partial x^2} + u\left\{1 - \frac{1}{\lambda}\int_{-\infty}^{\infty} \phi\left(\frac{y-x}{\lambda}\right) u(y,t)\mathrm{d}y\right\}. \tag{1}$$

As shown in [1], this has permanent form travelling wave solutions for all wavespeeds greater than or equal to two, with this minimum wavespeed fixed by the behaviour of the solution when $u \ll 1$. The linearisation of (1) when $u \ll 1$ is the same as that of the local Fisher-KPP equation,

$$\frac{\partial u}{\partial t} = \frac{\partial^2 u}{\partial x^2} + u(1-u), \tag{2}$$

and the minimum wavespeed exists for the same reason, namely that no strictly positive travelling wave solutions exist for wavespeed less than two. A more general form of nonlocal reaction diffusion equation is

$$\frac{\partial u}{\partial t} = \frac{\partial^2 u}{\partial x^2} + u^\alpha\left\{1 - \frac{1}{\lambda}\int_{-\infty}^{\infty} \phi\left(\frac{y-x}{\lambda}\right) u^\beta(y,t)\mathrm{d}y\right\} - \gamma u, \tag{3}$$

with $\alpha \geqslant 1, \beta \geqslant 1$ and $\gamma > 0$, which is discussed in detail in [3], and a derivation for population modelling is given based on a kinetic transport formulation. The same equation can be used to model other phenomena, such as cell migration and cancer growth, see [5] wherein there is an extensive discussion of the use of nonlocal models in biology (for example [6–8]). It is clear from the discussion given in [3] that when $\gamma = 0$, the choice of α, β and the kernel $\phi(y)$ all strongly affect both the form and speed of travelling waves generated in initial value problems, as well as the existence of solutions that blow up in finite time.

In this paper, we study travelling wave solutions of the cubic NLFKPP ((3) with $\alpha = 2$, $\beta = 1, \gamma = 0$), which combines generic reaction degeneracy at low concentration with classical nonlocal effects, namely

$$\frac{\partial u}{\partial t} = \frac{\partial^2 u}{\partial x^2} + u^2\left\{1 - \frac{1}{\lambda}\int_{-\infty}^{\infty} \phi\left(\frac{y-x}{\lambda}\right) u(y,t)\mathrm{d}y\right\}, \tag{4}$$

for $(x,t) \in \mathbb{R} \times \mathbb{R}^+$. This is the simplest and most natural example to study from the family of equations given by (3) with a source term that is nonlinear when $u \ll 1$. A variant of this system, actually (3) with $\alpha = 2$ and $\beta = 1$, is studied in [9], where some results related to

(4) are discussed. We study (4) with a prescribed kernel $\phi(y)$ that is piecewise continuous, symmetric, nonnegative and nontrivial, integrable and nonincreasing for $y > 0$, has a finite derivative as $y \to 0^+$ and is normalised so that

$$\int_{-\infty}^{\infty} \phi(y)\mathrm{d}y = 1. \tag{5}$$

The parameter λ is the ratio of the nonlocal lengthscale associated with the kernel to the diffusive lengthscale. Since we will mainly be interested in the limit $\lambda \to 0$, it is useful to make the simple change of variable $y \mapsto x + \lambda y$, so that (4) becomes

$$\frac{\partial u}{\partial t} = \frac{\partial^2 u}{\partial x^2} + u^2\left\{1 - \int_{-\infty}^{\infty} \phi(y)\, u\,(x + \lambda y, t)\,\mathrm{d}y\right\}. \tag{6}$$

In this form it is clear that when $\lambda = 0$, (6) reduces to the local cubic Fisher-KPP equation,

$$\frac{\partial u}{\partial t} = \frac{\partial^2 u}{\partial x^2} + u^2(1 - u). \tag{7}$$

Apart from the applications described above, this equation arises naturally in chemical reaction theory in modelling cubic autocatalysis, in which two molecules of a substance are required to catalyse its production through $A + 2B \to 3B$ and the law of mass action applies, [2]. Equation (6) is a natural nonlocal extension.

Since the reaction terms in equations (4) to (7) have a nonlinear dependence on u, there is a sense in which they are all degenerate, since a linear perturbation would fundamentally affect the form of their solutions, or from another point of view, they represent bifurcation points in an extended system of equations. An example of this is the bistable nonlocal system

$$\frac{\partial u}{\partial t} = \frac{\partial^2 u}{\partial x^2} + u\,(u - \theta)\left\{1 - \int_{-\infty}^{\infty} \phi(y)\, u\,(x + \lambda y, t)\,\mathrm{d}y\right\}, \tag{8}$$

which is studied in [10] for $0 < \theta < 1$. In this case there is a unique (up to translation) wavespeed and travelling wave solution. When $\theta = 0$, we recover (6) for which there is a unique exponentially-decaying travelling wave solution along with a family of algebraically-decaying travelling wave solutions, as discussed below. For $\theta < 0$, we would expect a one-parameter family of exponentially-decaying travelling wave solutions with wavespeed $c \geqslant 2\sqrt{-\theta}$, since the reaction term is qualitatively-similar to the quadratic NLFKPP equation, (1), although this has not to our knowledge been studied. A different unfolding, at least of the local equation (7), is provided by various versions of the Allen–Cahn equation, for example,

$$\frac{\partial u}{\partial t} = \frac{\partial^2 u}{\partial x^2} + \mu - bu + au^3 - u^5, \tag{9}$$

[11]. Through the addition of more structure to the reaction term, this allows an even wider range of wavefront solutions to exist, with (7) as a bifurcation point. Including nonlocal effects in (9) would be an interesting extension.

We consider general kernels as described above, and for which, in addition, the decay at long range satisfies the weak restriction,

$$\phi(y) \leqslant Ay^{-n} \quad \text{as } y \to \infty, \tag{10}$$

for some $n > 1$ and $A > 0$. The theory presented in sections 2 and 3 addresses the situation for such kernels in considerable generality. Typical kernels in this class are, for example, $\phi(y) =$

$\Phi_1(y) \equiv \frac{1}{2}\,\mathrm{e}^{-|y|}$ and $\phi(y) = \Phi_\infty(y) \equiv \frac{1}{2\sqrt{\pi}}\,\mathrm{e}^{-\frac{1}{4}y^2}$ ([12] gives a rationale for this notation) and $\phi(y) = \chi_n(y)$, with

$$\chi_n(y) \equiv \frac{\Gamma\left(\frac{1}{2}n\right)}{\sqrt{2n\pi}\,\Gamma\left(\frac{1}{2}n - \frac{1}{2}\right)}\left(1 + \frac{y^2}{2n}\right)^{-\frac{1}{2}n} \quad \text{for } n > 1. \tag{11}$$

Note that $\chi_n(y) \sim \Phi_\infty(y)$ as $n \to \infty$ when $|y| = o(\sqrt{n})$. This family of algebraically-decaying kernels is of particular interest, because we will find that the rate of decay of the kernel as $y \to \infty$ determines the size of the correction to the minimum wavespeed of the cubic local Fisher-KPP equation (corresponding to $\lambda = 0$) when $0 < \lambda \ll 1$. This correction is of $O(\lambda^4)$ for $n \geqslant 3$ and of $O(\lambda^{2(n-1)})$ for $1 < n \leqslant 3$. Another kernel of interest is the top hat kernel,

$$\phi(y) = \Phi_{\mathrm{H}}(y) \equiv \begin{cases} 1 & \text{for } |y| \leqslant \dfrac{1}{2}, \\ 0 & \text{otherwise}, \end{cases} \tag{12}$$

which has been discussed in [13]. Unlike the other kernels mentioned above, this kernel leads to the uniform steady state $u = 1$ of (6) being unstable, and we will discuss this further below.

To study permanent form travelling wave solutions of (6) we define a travelling wave coordinate $z = x - ct$, where $c > 0$ is a constant wavespeed to be determined. We seek a solution $u(x, t) = U(z)$, so that

$$U'' + cU' + U^2\left\{1 - \int_{-\infty}^{\infty}\phi(y)\,U\,(z + \lambda y)\,\mathrm{d}y\right\} = 0, \tag{13}$$

with $z \in \mathbb{R}$ and where a prime denotes $\mathrm{d}/\mathrm{d}z$. This nonlocal ordinary differential equation is to be solved subject to the conditions

$$U \geqslant 0, \quad z \in \mathbb{R}, \tag{14}$$

$$U \to 1 \quad \text{as } z \to -\infty, \tag{15}$$

$$U \to 0 \quad \text{as } z \to \infty. \tag{16}$$

When $\lambda = 0$, (13) becomes the ordinary differential equation

$$U'' + cU' + U^2(1 - U) = 0, \tag{17}$$

which was the subject of [2]. In [2] we showed that there is a minimum wavespeed $c_{\min} = \frac{1}{\sqrt{2}}$ such that a unique (up to translation) solution of (17) exists for all $c \geqslant c_{\min}$. Moreover, the minimum speed travelling wave is given analytically by

$$U = U_{\min}(z) \equiv \frac{1}{1 + \mathrm{e}^{c_{\min} z}}, \tag{18}$$

which decays exponentially fast as $z \to \infty$. For $c > c_{\min}$ the permanent form travelling wave solution has $U \sim c/z$ as $z \to \infty$. The existence of these two possible types of behaviour ahead of the wavefront, where $0 < U \ll 1$, can be deduced from a local analysis, but the minimum wavespeed is determined by the global behaviour of the solutions of (17) in the phase plane. This is in contrast to the quadratic Fisher-KPP equation, for which the minimum wavespeed is determined by the local behaviour of the solution as $z \to \infty$, where $0 < U \ll 1$. We also note that all travelling wave solutions of the quadratic and cubic Fisher-KPP equations are monotonically decreasing for $c > 0$. This is not the case for the nonlocal versions of these equations (see [1, 12] and below).

In section 2 we will show that, consistent with the above result for $\lambda = 0$, there exists a minimum wavespeed $c_{\min}(\lambda) > 0$ for each $\lambda > 0$. Specifically, we establish that the positive quadrant of the (λ, c) parameter space contains the open region $\mathcal{A} = \{(\lambda, c) \in \mathbb{R}^+ \times \mathbb{R}^+ : c > c_{\min}(\lambda)\}$ where, at each point (λ, c), there exists a travelling wave solution (and its translates) with $U(z;\ c, \lambda) \sim c/z$ as $z \to \infty$, whilst for each $(\lambda, c) \in \overline{\mathcal{A}} \backslash \mathcal{A}$ there exists a unique travelling wave solution (up to translation) with $U(z;\ c, \lambda) = O(\mathrm{e}^{-cz})$ as $z \to \infty$. We have not seen any numerical evidence which indicates that there are any travelling wave solutions at any other points $(\lambda, c) \in \mathbb{R}^+ \times \mathbb{R}^+$ other than those identified above, as is the case for the local problem, $\lambda = 0$.

In section 3 we examine the asymptotic solution of (13) to (16) when $\lambda \ll 1$, in other words, when the nonlocal interaction occurs over a small lengthscale and the travelling wave solutions are close to those of the local cubic Fisher-KPP equation. This confirms that an exponentially-decaying travelling wave solution only exists at $c = c_{\min}(\lambda)$ for λ sufficiently small. In section 4 we describe a numerical method to find the exponentially-decaying travelling wave solution of (13) to (16) and compare this with the asymptotic solution for $\lambda \ll 1$.

2. General theory

In this section we consider, for a given $D > 0$, at which wavespeeds $c > 0$ there exists a permanent form travelling wave. The approach will be focused in the phase plane of the nonlocal equation (13). We note that, although the phase plane does not have all the key properties that the corresponding phase plane for a similar local equation would have, it remains a useful setting to study this nonlocal variant. We begin with some preliminary results, which establish qualitative features, and, moreover, then combine to enable us to establish the main result, given in (R11). For this purpose it is convenient to introduce into equation (13) the scaled coordinate

$$\xi = \sqrt{D}z, \tag{19}$$

with $\sqrt{D} \equiv 1/\lambda$. Equation (13) then becomes, with now $U = U(\xi)$

$$DU_{\xi\xi} + vU_\xi + U^2\left\{1 - \int_{-\infty}^{\infty} \phi(y)\, U(\xi + y)\, \mathrm{d}y\right\} = 0, \quad \xi \in \mathbb{R}, \tag{20}$$

and v now being the scaled wavespeed,

$$v = \sqrt{D}c. \tag{21}$$

As discussed in the introduction, we will restrict attention in this section to symmetric kernels that are piecewise differentiable (and so bounded), integrable, nonincreasing on $(0, \infty)$ and nontrivial. Our intention is to focus on kernels characterised by a single lengthscale that represent intraspecies competition (by being nonnegative) for which the degree of competition decreases with separation. Other choices of kernel, for example, kernel functions that increase with separation for some ranges of separation, kernels that become negative (representing cooperation instead of competition) and asymmetric kernels (representing some asymmetry in the underlying system being modelled) may have a significant effect on the nature of the solutions, even for $\lambda \ll 1$. Our intention in the present paper is to focus on, in our view, the simplest possible family of kernels that extend the quadratic and cubic Fisher-KPP equations to have nonlocal competition.

A permanent form travelling wave solution with wavespeed $v > 0$, which we henceforth refer to as a PTW, is a solution to (20) that satisfies the conditions

$$U(\xi) \to \begin{cases} 1 & \text{as } \xi \to -\infty, \\ 0 & \text{as } \xi \to \infty \end{cases} \tag{22}$$

$$U(\xi) \geqslant 0 \quad \forall \xi \in \mathbb{R}. \tag{23}$$

To begin with, we first consider solutions to the nonlinear, nonlocal ordinary differential equation (NLODE) (20) that have $|U|$, $|U_\xi| \ll 1$ with $\xi \gg 1$. This is most readily achieved by examining the form of (20) in the (U, U_ξ) phase plane, local to the equilibrium point at $(U, U_\xi) = (0, 0)$. The form of (20) close to $(0, 0)$ is

$$DU_{\xi\xi} + vU_\xi + U^2 = 0 \quad \text{for } \xi \gg 1, \tag{24}$$

and we remark that this leading order form has reduced to a local, nonlinear form that is the same as that which characterises the behaviour for $U \ll 1$ in the local form of the equation (7). The structure of solutions to (24), in an open disc centred at $(0, 0)$ with sufficiently small radius, can be achieved rigorously via the centre manifold theorem (see for example [14, p 154]). The analysis of (24) establishes the existence of a stable manifold at $(0, 0)$ (corresponding to local eigenvalue $\mu = -v$) which has structure

$$U_\xi(U) \sim -vU \quad \text{(SM)} \tag{25}$$

with $|U| \ll \min(1, v^{-1})$, and a centre manifold at $(0, 0)$ (corresponding to local eigenvalue $\mu = 0$) which has structure

$$U_\xi(U) \sim -\frac{U^2}{v} \quad \text{(CM)} \tag{26}$$

with $|U| \ll \min(1, v)$. The local phase portrait is then constructed in the form illustrated in figures 1(a)–(c). Figure 1(a) shows the phase portrait when $v = 0$, a degenerate case in which no phase paths with $U > 0$ asymptote to $(0, 0)$ as $\xi \to \infty$. In figure 1(b) v is small enough that the stable manifold of $(0, 0)$, shown as a broken line, enters the region $U_\xi > 0$. In figure 1(c) v is large enough that the stable manifold of $(0, 0)$ has $U_\xi < 0$ globally.

We are now able to make the following observations.

(R1) There exists $\delta > 0$ (and small) such that, when $v \in [0, \delta]$, then every solution $(U(\xi), U_\xi(\xi))$ of ODE (24), and hence of NLODE (20), that has $(U(\xi), U_\xi(\xi)) \to (0, 0)$ as $\xi \to \infty$, corresponds to a phase path in figures 1(a) or (b), when $v = 0$ or $v \in (0, \delta]$ respectively, and so *cannot remain non-negative*.

(R2) At each $v = v_0 > 0$, each solution $(U(\xi, v_0), U_\xi(\xi, v_0))$ of NLODE (20) that remains bounded away from $(0, 0)$ as $\xi \to \infty$, also remains bounded away from $(0, 0)$ as $\xi \to \infty$ for each v in a sufficiently small neighbourhood of $v = v_0$. This is a consequence of continuous dependence of solutions to (20) on v at $v = v_0$, together with the structure of the phase portraits shown in figure 1.

(R3) At each $v = v_0 > 0$, any solution $(U(\xi, v_0), U_\xi(\xi, v_0))$ that has $\xi_0 \in \mathbb{R}$ such that $U(\xi_0, v_0) < 0$ has a corresponding $\xi_v \in \mathbb{R}$ such that $U(\xi_v, v) < 0$ for each v in a sufficiently small neighbourhood of $v = v_0$. This, again, is a consequence of continuous dependence of solutions to (20) on v at $v = v_0$.

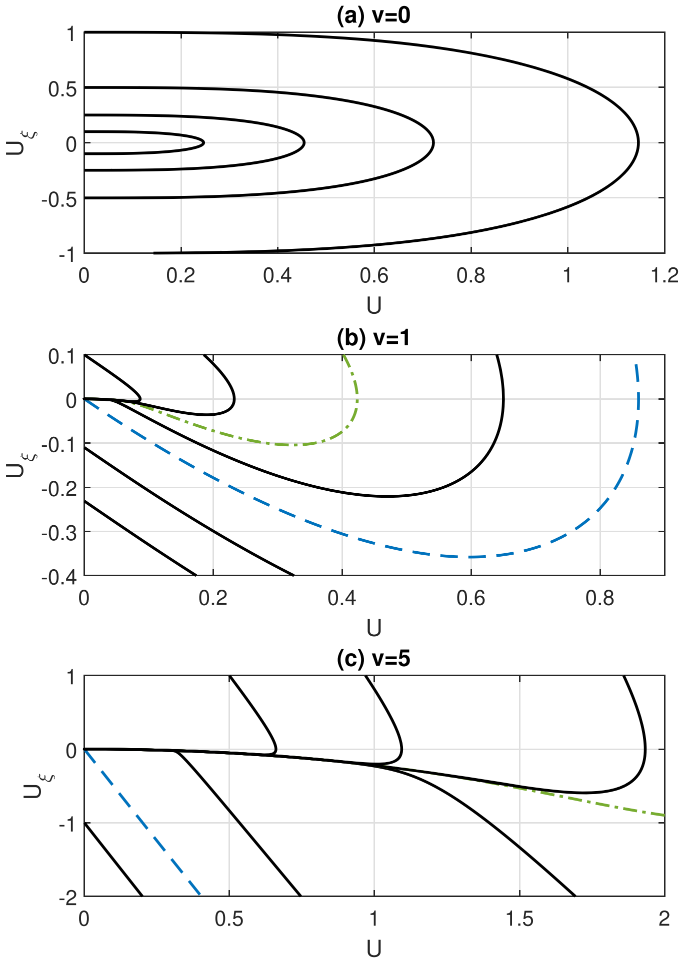

Figure 1. The local phase portrait for (20) in the (U, U_ξ) phase plane when $D = 1$, calculated from (24) using 'ode45' in Matlab for (a) $v = 0$, (b) $v = 1$ and (c) $v = 5$. The stable and centre manifolds of (0, 0) are shown as broken blue and dot-dashed green lines, respectively.

It is now straightforward to establish that solutions to NLODE (20) with $v > 0$, say $(U(\xi, v), U_\xi(\xi, v))$ that have $(U(\xi, v), U_\xi(\xi, v)) \to (0, 0)$ as $\xi \to \infty$ are (via the linearisation and centre manifold theorems) given by, via (25) and (26),

$$(U(\xi, v), U_\xi(\xi, v)) \sim \left(\frac{Av}{(A\xi + 1)} + B\,\mathrm{e}^{-v\xi}, -\frac{A^2 v}{(A\xi + 1)^2} - Bv\,\mathrm{e}^{-v\xi} \right) \tag{27}$$

as $\xi \to \infty$. Here A and B are two free, real constants, with

$$A \geqslant 0 \tag{28}$$

and

$$B \neq 0 \quad \text{when} \quad A = 0. \tag{29}$$

There are three possibilities, namely:

- $A = 0$, $B \neq 0$—gives the solution (and its translations in ξ) corresponding to the local stable manifold at (0, 0).
- $A > 0$, $B = 0$—gives the solution (and its translations in ξ) corresponding to the local centre manifold at (0, 0).
- $A > 0$, $B \neq 0$—gives the solutions (and their translations in ξ) corresponding to phase paths that enter (0, 0) asymptotic to the local centre manifold (in the half plane $U > 0$) at (0, 0).

The next preliminary is to consider solutions to NLODE (20) that, in the (U, U_ξ) phase plane, have $(U(\xi, v), U_\xi(\xi, v)) \to (1, 0)$ as $\xi \to -\infty$. The local solutions satisfy the linearised approximation

$$D\bar{U}_{\xi\xi} + v\bar{U}_\xi - \int_{-\infty}^{\infty} \phi(y)\bar{U}(\xi + y)\mathrm{d}y = 0 \quad \text{for } (-\xi) \gg 1, \tag{30}$$

with $\bar{U} = U - 1$. This is justified by the linearisation theorem (see, for example, [15]). We observe that here the local behaviour is linear, but retains a nonlocal term, unlike the corresponding approximation local to (0, 0). The existence and nature of solutions to (30) that have

$$\bar{U}(\xi), \bar{U}_\xi(\xi) \to 0 \quad \text{as } \xi \to -\infty, \tag{31}$$

can be examined by considering solutions to the global, linear, nonlocal problem

$$D\bar{U}_{\xi\xi} + v\bar{U}_\xi - \int_{-\infty}^{\infty} \phi(y)\bar{U}(\xi + y)\mathrm{d}y = \delta(\xi), \quad \text{for } \xi \in \mathbb{R}, \tag{32}$$

$$\bar{U}(\xi), \bar{U}_\xi(\xi) \to 0 \quad \text{as } |\xi| \to \infty, \tag{33}$$

with $\delta : \mathbb{R} \to \mathbb{R}$ being the usual Dirac delta function, and

$$\bar{U} \in C^2\big(\mathbb{R}\backslash\{0\}\big) \cap C(\mathbb{R}) \cap L^1(\mathbb{R}). \tag{34}$$

The problem (32) to (34) can be analysed directly via Fourier theory. With $\phi : \mathbb{R} \to \mathbb{R}$ as discussed earlier, it is readily established that the solution to (32) to (34) is uniquely determined as

$$\bar{U}(\xi, v) = -\frac{1}{2\pi}\int_{-\infty}^{\infty} \Big(Dk^2 + \mathrm{i}kv + \hat{\phi}(k)\Big)^{-1} \mathrm{e}^{-\mathrm{i}k\xi}\,\mathrm{d}k \tag{35}$$

for all $(\xi, v) \in \mathbb{R} \times \mathbb{R}^+$. Here $\hat{\phi} : \Omega \to \mathbb{C}$, with $\Omega \subseteq \mathbb{C}$ being a suitable complex domain, is the Fourier transform of $\phi : \mathbb{R} \to \mathbb{R}$, given by

$$\hat{\phi}(k) = \int_{-\infty}^{\infty} \phi(s)\mathrm{e}^{\mathrm{i}ks}\,\mathrm{d}s, \tag{36}$$

for all $k \in \Omega$. We remark that $\mathbb{R} \subseteq \Omega$. In addition, we observe that

$$\hat{\phi}^*(k) = \hat{\phi}(-k^*) \quad \forall\, k \in \Omega, \tag{37}$$

$$\hat{\phi}(k) = \hat{\phi}(-k) \quad \forall\, k \in \mathbb{R}, \tag{38}$$

using the properties of ϕ. It follows from (38) that

$$\hat{\phi}(k) \in \mathbb{R} \quad \forall\, k \in \mathbb{R}, \tag{39}$$

with

$$\hat{\phi}(0) = 1 \tag{40}$$

and

$$\hat{\phi}(k) = o(k^{-1}) \quad \text{as } |k| \to \infty \quad \text{in } \mathbb{R}. \tag{41}$$

Moreover, $\hat{\phi} \in C(\Omega) \cap L^\infty(\Omega)$. On using (36) to (41) in (35) it is readily established that

$$\bar{U} \in C^{2,0}(\mathbb{R}^- \times \mathbb{R}^+), \tag{42}$$

as required. It is a direct consequence of the Riemann–Lebesgue lemma, with (36) to (41), that, as required,

$$\bar{U}(\xi, v), \bar{U}_\xi(\xi, v) \to 0 \quad \text{as } \xi \to -\infty \tag{43}$$

at each $v \in \mathbb{R}^+$. We write

$$\bar{U}(\xi, v) \sim \bar{U}_{-\infty}(\xi, v) \quad \text{as } \xi \to -\infty \tag{44}$$

at each $v \in \mathbb{R}^+$, noting that $\bar{U}_{-\infty}(\cdot, v)$ will depend continuously on $v \in \mathbb{R}^+$. We observe directly from (35) with (36) to (41) that we may take

$$\bar{U}_{-\infty}(\xi, v) \sim -v^{-1}\,\mathrm{e}^{v^{-1}\xi} \quad \text{as } v \to \infty, \tag{45}$$

with $(-\xi) \gg v$. In general, when $v = O(1)^+$, the structural form of $\bar{U}_{-\infty}(\xi, v)$ will depend upon the decay rate and regularity of $\phi(\xi)$. We are able to conclude that, for each $v > 0$, there exists an unstable manifold for NLODE (20) at the equilibrium point (1, 0) (not necessarily the only one), which has the parametric form, in the (U, U_ξ) phase plane,

$$(U, U_\xi) \sim \left(1 + \bar{U}_{-\infty}(\xi, v), \bar{U}'_{-\infty}(\xi, v)\right) \quad \text{as } \xi \to -\infty, \tag{46}$$

with $v \in \mathbb{R}^+$ fixed. This unstable manifold deforms continuously with $v \in \mathbb{R}^+$ and, in particular, has the form

$$U_\xi \sim v^{-1}(U - 1) \quad \text{as } U \to 1, \tag{47}$$

with $v \gg 1$, via (45).

The question we now wish to address is, for which values of $v > 0$ (if any) does the *specific unstable manifold* at (1, 0) identified above in (46) (we note that the nonlocal term may give rise to further stable manifolds at the equilibrium point (1, 0), and possibly a countably infinite number; however, for the specific argument we develop below, we choose only to focus on that stable manifold which has been identified above) connect to the stable manifold or is asymptotic to the centre manifold, at (0, 0), with the corresponding phase path remaining in the right half plane, in the (U, U_ξ) phase plane. For convenience, we now introduce the following terminology. We denote the phase path of NLODE (20) that leaves the equilibrium point (1, 0) on the unstable manifold (46) as $\mathcal{S}(v)$. When $\mathcal{S}(v)$ remains in the right half plane and connects with the stable manifold at (0, 0), we refer to this as a PTW *of type E*. Alternatively, when $\mathcal{S}(v)$ remains in the right half plane and connects to a phase path asymptotic to the centre manifold at (0, 0), we refer to this as a PTW *of type A*. When neither of these two cases pertain, we say that $\mathcal{S}(v)$ is a non PTW path. Roughly speaking, in what follows we will use continuous dependence of the specific stable manifold $\mathcal{S}(v)$ on v to establish that if a PTW connection exists at a given v, then this connection persists in an interval containing this value of v. We can then examine the nature of this interval. Finally, the existence of such an interval is established by demonstrating constructively that indeed, for all v sufficiently large, the stable manifold $\mathcal{S}(v)$ does indeed form a PTW connection.

We now have the following results:

(R4) There is a $\delta > 0$ (which may depend upon $D > 0$) such that no PTW exists for wavespeeds $v \in (0, \delta]$.

Proof. This follows directly from (R1), in relation to non-negativity.

We now restrict attention to the existence of PTW of type A or type E.

(R5) Suppose that no PTW of type A or type E exists at $v = v^* > 0$. Then there exists $\delta' > 0$ (which may depend upon v^* and D) such that no PTW of type A or type E exists at each $v \in (v^* - \delta', v^* + \delta')$.

Proof. Under the conditions in the statement, $\mathcal{S}(v^*) \cap \{(U, U_\xi) : U \geqslant 0\}$ must remain bounded away from (0, 0) in figure 1. The continuous dependence of $\mathcal{S}(v)$ on v at $v = v^*$ then guarantees that there is a $\delta' > 0$ (which may depend upon v^* and D) such that $\mathcal{S}(v) \cap \{(U, U_\xi) : U \geqslant 0\}$ remains bounded away from (0, 0) for each $v \in (v^* - \delta', v^* + \delta')$, and the result follows.

(R6) Let $U = U_T : \mathbb{R} \to \mathbb{R}$ be a PTW, then $U_T \in C^\omega(\mathbb{R})$.

Proof. $U = U_T \in C^\omega(\mathbb{R})$ follows from $U_T \in C^2(\mathbb{R})$ and then induction on equation (20), using the chain rule and observing that $f(X, Y) = X^2(1 - Y)$ is analytic in $\mathbb{R}^2$.

(R7) Let $U = U_T : \mathbb{R} \to \mathbb{R}$ be a PTW with wavespeed $v > 0$. Then $U_T(\xi) > 0$ for all $\xi \in \mathbb{R}$.

Proof. Suppose that there is $\xi_0 \in \mathbb{R}$ such that $U_T(\xi_0) = 0$, then, via (23), $U_T'(\xi_0) = 0$, and so, using (20), (R6) and induction, we have $U_T^{(n)}(\xi_0) = 0$ for $n = 2, 3, 4 \ldots$. Therefore, as $U_T \in C^\omega(\mathbb{R})$, then $U_T(\xi) = 0$ for all $\xi \in \mathbb{R}$, which contradicts (22), and the result follows.

We are now able to establish the following.

(R8) Suppose there is a PTW of type A with wavespeed $v = v_A > 0$. Then there is $\delta_A > 0$ (which may depend on both v_A and D) such that a PTW of type A exists for each wavespeed $v \in (v_A - \delta_A, v_A + \delta_A)$.

Proof. At $v = v_A$, then $\mathcal{S}(v)$ enters (0, 0) asymptotic to the centre manifold with, in particular, $\mathcal{S}(v_A)$ remaining in $\{(U, U_\xi) : U > 0\}$ for all $\xi \in \mathbb{R}$ via (R7). Specifically, as $\mathcal{S}(v_A)$ is a smooth curve in the (U, U_ξ) phase plane connecting (1, 0) to (0, 0) in $\{(U, U_\xi) : U > 0\}$, then $\mathcal{S}(v_A)$ is bounded away from $\{(0, U_\xi) : |U_\xi| > l\}$ for each fixed $l > 0$. This, together with the structure at (0, 0) in figure 1(c), and the continuous dependence of $\mathcal{S}(v)$ on v at $v = v_A$, guarantees that there is a $\delta_A > 0$ (which may depend on v_A and D) such that $\mathcal{S}(v)$ connects (1, 0) to (0, 0) at each $v \in (v_A - \delta_A, v_A + \delta_A)$ with, moreover, $\mathcal{S}(v)$ in $\{(U, U_\xi) : U > 0\}$. Thus there is a PTW of type A at each $v \in (v_A - \delta_A, v_A + \delta_A)$ as required.

We next consider PTWs for fixed $D > 0$, when v is large. Thus we move directly to problem (20), (22) and (23), with fixed D, as $v \to \infty$. In this limit, a balance of terms in NLODE (20) requires a scaling of the independent variable, introducing ζ so that,

$$\xi = v\zeta. \tag{48}$$

In terms of ζ, (20) becomes

$$\bar{D}U_{\zeta\zeta} + U_\zeta + U^2\left(1 - \int_{-\infty}^{\infty}\phi(y)U\left(\zeta + \frac{y}{v}\right)\mathrm{d}y\right) = 0 \quad \text{for } \zeta \in \mathbb{R}, \tag{49}$$

with

$$\bar{D} = Dv^{-2}. \tag{50}$$

We now estimate the nonlocal term in (49) with $v \gg 1$. We write

$$\begin{aligned}\int_{-\infty}^{\infty}\phi(y)U\left(\zeta + \frac{y}{v}\right)\mathrm{d}y &= \int_{-\sqrt{v}}^{\sqrt{v}}\phi(y)U\left(\zeta + \frac{y}{v}\right)\mathrm{d}y + o(1)\\ &\sim U(\zeta)\int_{-\sqrt{v}}^{\sqrt{v}}\phi(y)\mathrm{d}y \sim U(\zeta) \quad \text{as } v \to \infty.\end{aligned} \tag{51}$$

On using (51) and (50) in (49), we obtain, when

$$v \gg \max(1, \sqrt{D}), \tag{52}$$

that

$$U_\zeta \sim -U^2(1 - U). \tag{53}$$

On replacing ζ with the original variable, ξ, we immediately obtain an approximation to $\mathcal{S}(v)$ in the (U, U_ξ) phase plane, when v satisfies (52), as

$$U_\xi \sim v^{-1}U^2(1 - U) \quad \text{with } 0 \leqslant U \leqslant 1. \tag{54}$$

We remark that (54) satisfies (45) (as it should) and also satisfies (26), which ensures that for each v satisfying (52), the corresponding $\mathcal{S}(v)$ is a PTW of type A. Thus, we have established

(R9) For each $D > 0$ there is a $v_\infty > 0$ (which may depend upon D) such that a PTW of type A exists for each $v \in (v_\infty, \infty)$.

Proof. This follows from the preceding argument.

We now introduce, for each fixed $D > 0$, the set $\mathcal{A}(D) \subset \mathbb{R}^+$ (via (R1)), where

$$\mathcal{A}(D) = \{V \in \mathbb{R}^+ : \exists \quad \text{a (PTW) of type A for each } v \geqslant V\}. \tag{55}$$

We observe from (R1) that $\mathcal{A}(D) \subseteq (\delta, \infty)$, with $\delta > 0$ as given in (R1) (and which may depend upon D). Moreover, it follows from (R9) that

$$\mathcal{A}(D) \neq \emptyset. \tag{56}$$

Now let

$$\alpha(D) = \inf \mathcal{A}(D). \tag{57}$$

As a consequence of (R1), we have

$$\alpha(D) \geqslant \delta, \tag{58}$$

and, by definition,

$$\mathcal{A}(D) = (\alpha(D), \infty), \tag{59}$$

or

$$\mathcal{A}(D) = [\alpha(D), \infty). \tag{60}$$

Now, suppose $\alpha(D) \in \mathcal{A}(D)$, then there is a PTW of type A at wavespeed $v = \alpha(D)$. However, it then follows from (R8) that $\alpha(D) \neq \inf \mathcal{A}(D)$. This contradiction establishes that $\alpha(D) \notin \mathcal{A}(D)$, and so $\mathcal{A}(D)$ is given by (59). Now suppose that no PTW of type E exists at $v = \alpha(D)$, then it follows from (R5) that no PTW of type A exists for v in a neighbourhood of $v = \alpha(D)$, which contradicts (59). We can conclude that there exists a PTW of type E at wavespeed $v = \alpha(D)$. We have established,

(R10) For each $D > 0$, there exists a PTW (corresponding to a connection on $\mathcal{S}(v)$ in the phase plane) for each propagation speed $v \in [\alpha(D), \infty)$. This is a PTW of type A for $v \in (\alpha(D), \infty)$ and a PTW of type E for $v = \alpha(D)$.

We now introduce the set $\mathcal{N}(D)$, which, for fixed $D > 0$, is defined as

$$\mathcal{N}(D) = \{V \in \mathbb{R}^+ : \text{No (PTW) exists for wavespeeds } v \in (0, V]\}. \tag{61}$$

As a consequence of (R1),

$$\mathcal{N}(D) \neq \emptyset, \tag{62}$$

whilst $\mathcal{N}(D)$ is bounded above, via (R10). We set

$$\beta(D) = \sup \mathcal{N}(D), \tag{63}$$

and observe from (R10) that

$$\beta(D) \leqslant \alpha(D). \tag{64}$$

Now, if $\beta(D) \in \mathcal{N}(D)$, then no PTW exists at wavespeed $v = \beta(D)$. However it then follows from either of (R2) or (R3) that no PTW exists for wavespeeds v in a neighbourhood of $v = \beta(D)$, which contradicts (63). We can conclude that

$$\beta(D) \notin \mathcal{N}(D), \tag{65}$$

and so,

$$\mathcal{N}(D) = (0, \beta(D)). \tag{66}$$

We note from (65) that a PTW must exist at wavespeed $v = \beta(D)$. If this PTW corresponds to a phase plane connection on $\mathcal{S}(v)$, then it follows from (66) and (R8) that this must be a PTW of type E. We have established

(R11) For each $D > 0$ there exists $\alpha(D)$ and $\beta(D)$, with $0 < \beta(D) \leqslant \alpha(D)$ such that

1. No PTW exists at each wavespeed $v \in (0, \beta(D))$.
2. A PTW of type E exists at wavespeeds $v = \beta(D)$ and $v = \alpha(D)$.
3. A PTW of type A exists at each wavespeed $v \in (\alpha(D), \infty)$.

We remark that a detailed numerical exploration, at least for the kernels discussed in the introduction, leads us to the following conjectures,

(C1) $\alpha(D) = \beta(D)$

(C2) The PTWs identified in (R11), on the connection $\mathcal{S}(v)$ in the phase plane, are (up to translations in ξ) the only PTWs.

These conjectures are further supported by the analysis in the next section, relating to PTWs when $D \gg 1$ ($\lambda \ll 1$).

To complete the analysis, let $U = U_T^{(A)}(\xi, v)$ be a PTW of type A with wavespeed v; it follows from (27) that

$$U_T^{(A)}(\xi, v) \sim \frac{v}{\xi} \quad \text{as } \xi \to \infty. \tag{67}$$

However, when $U = U_T^{(E)}(\xi, v)$ is a PTW of type E, then,

$$U_T^{(E)}(\xi, v) \sim C_\infty(v)\mathrm{e}^{-v\xi} \quad \text{as } \xi \to \infty, \tag{68}$$

with $C_\infty(v) > 0$ being a globally-determined constant (depending, in general, on v). The quantitative details of the behaviour of a PTW as $\xi \to -\infty$ depend upon the kernel under consideration. However, there are just two possibilities for the kernels under consideration here, namely for a PTW at $(D, v) \in \mathbb{R}^+ \times \mathbb{R}^+$, then either

(a) $U_T(\xi, v)$ has purely exponential decay to unity as $\xi \to -\infty$,

(b) $U_T(\xi, v)$ has harmonic oscillatory decay to unity as $\xi \to -\infty$.

As an example, we make the calculation for the top hat kernel of unit base. We can establish whether (a) or (b) occurs at a given $(D, v) \in \mathbb{R}^+ \times \mathbb{R}^+$ via the earlier linearised analysis in (30) to (45). In this case, we have

$$\hat{\phi}(k) = \begin{cases} \dfrac{2}{k} \sin \dfrac{1}{2}k & \text{for } k \in \mathbb{C}\backslash\{0\}, \\ 1 & \text{for } k = 0. \end{cases} \tag{69}$$

After some detailed, but straightforward calculations, we establish that case (a) occurs for $(D, v) \in \mathcal{F}$ and case (b) occurs for $(D, v) \in \mathcal{G}$, where $\mathcal{F}, \mathcal{G} \subset \mathbb{R}^+ \times \mathbb{R}^+$, which are separated by the finite curve $\mathcal{C}$, which is a monotone curve from the point $(0, v_0)$ to the point $(0, D_0)$, where

$$D_0 = \frac{1}{\lambda^2} \cosh \frac{1}{2}\lambda - \frac{4}{\lambda^3} \sinh \lambda, \tag{70}$$

$$\tanh \frac{1}{2}\lambda = \frac{1}{6}\lambda, \quad \lambda > 0, \tag{71}$$

which gives $D_0 \approx 9.28 \times 10^{-2}$, and

$$v_0 = \frac{6}{\lambda^2} \sinh \frac{1}{2}\lambda - \frac{1}{\lambda} \cosh \frac{1}{2}\lambda, \tag{72}$$

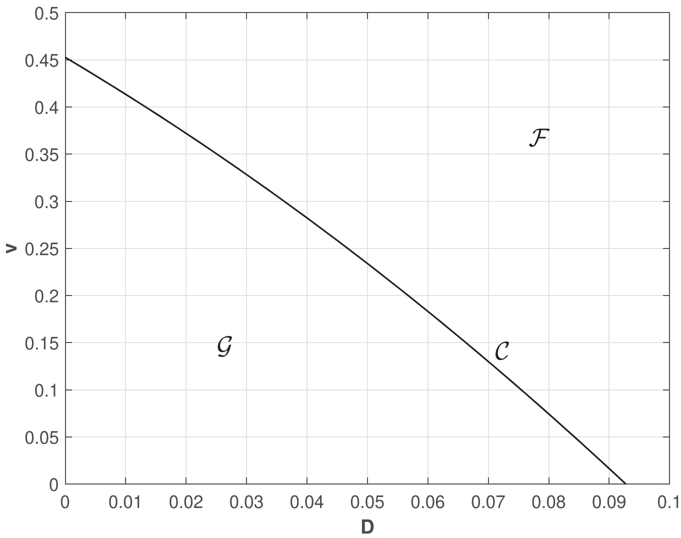

Figure 2. The regions $\mathcal{F}$, $\mathcal{G}$, separated by the curve $\mathcal{C}$ in the (v, D)-plane.

$$\tanh \frac{1}{2}\lambda = \frac{1}{4}\lambda, \tag{73}$$

which gives $v_0 \approx 0.453$. The dividing curve is given parametrically by

$$D = \frac{1}{\lambda^2} \cosh \frac{1}{2}\lambda - \frac{4}{\lambda^3} \sinh \lambda, \tag{74}$$

$$v = \frac{6}{\lambda^2} \sinh \frac{1}{2}\lambda - \frac{1}{\lambda} \cosh \frac{1}{2}\lambda, \tag{75}$$

for $0 < \lambda^- \leqslant \lambda \leqslant \lambda^+$, where $\lambda^- \approx 3.830$ is the solution to (71) and $\lambda^+ \approx 5.970$ is the solution to (73). The region $\mathcal{G}$ is that which has finite area. The regions $\mathcal{F}$ and $\mathcal{G}$ and the curve $\mathcal{C}$ are shown in figure 2.

3. Asymptotic solution for $\lambda \ll 1$

As we have seen, when $\lambda = 0$ (13) becomes (17), whose solutions have minimum wavespeed $c_{\min} = 1/\sqrt{2}$. In this section we will construct the asymptotic minimum wavespeed solution when $\lambda \ll 1$.

3.1. Case 1: $\phi(y) = o(y^{-3})$ as $y \to \infty$

When $\lambda \ll 1$ it is natural to Taylor expand the convolution term in (13),

$$\phi * U(z) \equiv \int_{-\infty}^{\infty} \phi(y)\, U(z + \lambda y)\, \mathrm{d}y, \tag{76}$$

as

$$\phi * U(z) = U(z) + \lambda^2 k_2 U'''(z) + \lambda^4 k_4 U'''(z) + O(\lambda^6), \tag{77}$$

where

$$k_n \equiv \frac{1}{n!}\int_{-\infty}^{\infty} y^n \phi(y)\mathrm{d}y.$$

Note that, by the symmetry of $\phi(y)$, k_n is zero when n is odd. The asymptotic expansion (77) is valid *provided* that the kernel is sufficiently small when $y = O(\lambda^{-1})$. This is the case for exponentially-decaying kernels, but for algebrically-decaying kernels we need to be more careful in our treatment of (76) as $\lambda \to 0$, which is described in section 3.2. In this section we use (77) to construct the minimum wavespeed asymptotic solution.

We begin by expanding

$$U(z) = U_0(z) + \lambda^2 U_1(z) + \lambda^4 U_2(z) + O(\lambda^6), \qquad c = c_0 + \lambda^2 c_1 + \lambda^4 c_2 + O(\lambda^6),$$

and proceed by substituting into (13) to be solved subject to (15), the minimum wavespeed condition

$$U = O(\mathrm{e}^{-cz}) \quad \text{as } z \to \infty, \tag{78}$$

and also

$$U = \frac{1}{2} \quad \text{at } z = 0, \tag{79}$$

to fix the phase of the solution.

At leading order we obtain $c_0 = 1/\sqrt{2}$ and $U_0 = U_{\min}(z)$. At $O(\lambda^2)$,

$$U_1'' + c_0 U_1' + U_0(2 - 3U_0)U_1 = -c_1 U_0' + k_2 U_0^2 U_0'', \tag{80}$$

to be solved subject to

$$U_1 \to 0 \quad \text{as } z \to -\infty, \quad U_1 = O(z\,\mathrm{e}^{-c_0 z}) \quad \text{as } z \to \infty, \quad U_1(0) = 0. \tag{81}$$

Since the homogeneous part of (80) is satisfied by $U_0'(z)$, we can solve (80) using variation of parameters to obtain

$$\begin{aligned} U_1 &= A_1 U_0'(z)\int_0^z \frac{\mathrm{e}^{-c_0 q}}{U_0'(q)^2}\,\mathrm{d}q + B_1 U_0'(z) \\ &\quad - U_0'(z)\int_0^z \frac{\mathrm{e}^{-c_0 q}}{U_0'(q)^2}\int_0^q \mathrm{e}^{c_0 s} U_0'(s)\left\{c_1 U_0'(s) - k_2 U_0(s)^2 U_0''(s)\right\}\mathrm{d}s\,\mathrm{d}q, \end{aligned}$$

with A_1 and B_1 constants to be determined. The phase condition, (81) (c), shows that $B_1 = 0$, and the far field condition (81) (a) shows that A_1 must be chosen so that

$$U_1 = -U_0'(z)\int_0^z \frac{\mathrm{e}^{-c_0 q}}{U_0'(q)^2}\int_{-\infty}^q \mathrm{e}^{c_0 s} U_0'(s)\left\{c_1 U_0'(s) - k_2 U_0(s)^2 U_0''(s)\right\}\mathrm{d}s\,\mathrm{d}q.$$

Finally, the far field condition (81) (b) requires that

$$\int_{-\infty}^{\infty} \mathrm{e}^{c_0 s} U_0'(s)\left\{c_1 U_0'(s) - k_2 U_0(s)^2 U_0''(s)\right\}\mathrm{d}s = 0, \tag{82}$$

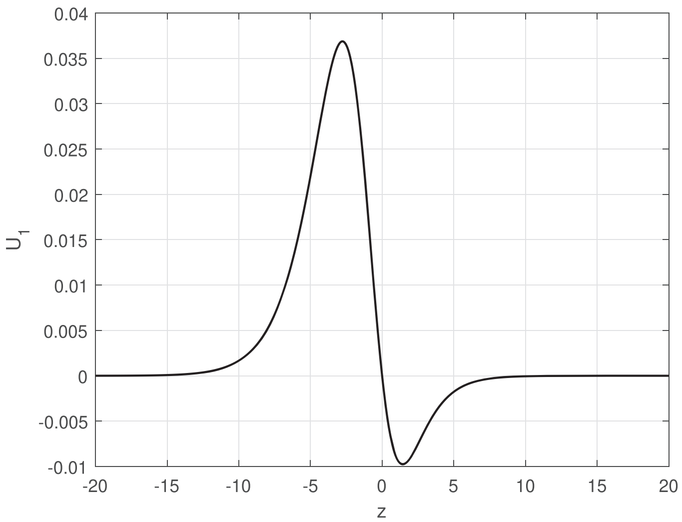

Figure 3. The correction to the leading order solution, U_1, given by (83) with $k_2 = 1$.

which determines c_1. The symmetry properties of U_0 show that $\mathrm{e}^{c_0 s} U_0'(s) U_0(s)^2 U_0''(s)$ is an odd function so that its integral vanishes, and hence that $c_1 = 0$. In fact, all of the integrals can be evaluated analytically using computer algebra, and we find that

$$U_1 = \frac{1}{24} k_2 \,\mathrm{sech}^2\left(\frac{z}{2\sqrt{2}}\right)\left[\tanh\left(\frac{z}{2\sqrt{2}}\right) + 2\,\log\left\{\frac{1}{2}\left(1 + \mathrm{e}^{-z/\sqrt{2}}\right)\right\}\right], \qquad (83)$$

which is plotted in figure 3. The asymmetry of U_1 leads, for λ sufficiently large, to a solution with an incipient local maximum behind the wavefront.

In order to determine c_2, which we now see gives the correction to c at $O(\lambda^4)$, we note that, at that order,

$$U_2'' + c_0 U_2' + U_0(2 - 3U_0)U_2 = -c_2 U_0' + F(z), \qquad (84)$$

with

$$F(z) \equiv -U_1^2 + 3U_0 U_1^2 + k_2\left(U_0^2 U_1'' + 2U_0 U_1 U_0''\right) + k_4 U_0^2 U_0''''.$$

Strictly speaking, we need $\phi(y) = o(y^{-5})$ as $y \to \infty$ for $k_4 \equiv \frac{1}{24}\int_{-\infty}^{\infty} y^4 \phi(y)\mathrm{d}y$ to exist, but we shall show in section 3.2 that the results below follow provided that $\phi(y) = o(y^{-3})$ as $y \to \infty$. Solving (84) leads to a condition analogous to (82), namely

$$\int_{-\infty}^{\infty} \mathrm{e}^{c_0 s} U_0'(s)\{c_2 U_0'(s) - F(s)\}\mathrm{d}s = 0,$$

and hence

$$c_2 = \int_{-\infty}^{\infty} \mathrm{e}^{c_0 s} U_0'(s) F(s)\mathrm{d}s \Big/ \int_{-\infty}^{\infty} \mathrm{e}^{c_0 s} U_0'(s)^2 \mathrm{d}s \qquad (85)$$

Since $\mathrm{e}^{c_0 s}U_0^2U_0'U_0''''$ is antisymmetric, the coefficient of k_4 in the numerator is zero. The remaining integrals can be calculated using symbolic algebra, and we find that

$$\begin{aligned} c_2 &= \sqrt{2}\left\{\frac{83-140\log 2}{58\,800} + k_2\left(\frac{-319+420\log 2}{176\,400}\right)\right\} \\ &\approx -3.38\times 10^{-4} - 2.24\times 10^{-4}k_2 < 0. \end{aligned} \tag{86}$$

Note that $k_2 = 1$ for both $\phi = \frac{1}{2}\,\mathrm{e}^{-|y|}$ and $\phi = \frac{1}{2\sqrt{\pi}}\,\mathrm{e}^{-\frac{1}{4}y^2}$, so that c_2 is typically numerically very small, making the correction $c - \frac{1}{\sqrt{2}} = c_2\lambda^4 + O(\lambda^6)$ numerically small and negative even for moderately small values of λ for these rapidly-decaying kernels. For the algebraically-decaying kernels given by (11), $k_2 = n/(n-3)$, consistent with the fact that, as we shall see in section 3.2, the order of the correction changes as $n \to 3^+$.

3.2. Case 2: $\phi(y) \gg y^{-3}$ as $y \to \infty$

In order to approximate the convolution term (76) when the kernel decays slowly as $y \to \infty$, it is helpful to rewrite it as

$$\phi{*}U(z) = U(z) + \int_0^\infty \phi(\bar{y})G(U, z, \lambda\bar{y})\mathrm{d}\bar{y}, \tag{87}$$

where

$$G(U, z, y) \equiv U(z+y) - 2U(z) + U(z-y).$$

Observe that $G(U, z, y) \sim y^2U''(z)$ as $y \to 0$. We will also assume that

$$\phi(y) \sim a_0 y^{-n}, \quad \text{as } y \to \infty,$$

with $a_0 > 0$. In order to make careful use of these approximations in (87), we rewrite it as

$$\phi{*}U(z) = U(z) + \int_0^{\psi(\lambda)} \phi(\bar{y})G(U, z, \lambda\bar{y})\mathrm{d}\bar{y} + \frac{1}{\lambda}\int_{\lambda\psi(\lambda)}^\infty \phi\left(\frac{y}{\lambda}\right)G(U, z, y)\mathrm{d}y, \tag{88}$$

where $\psi(\lambda)$ is chosen so that $1 \ll \psi \ll \lambda^{-1}$ and hence $\lambda \ll \lambda\psi \ll 1$. By ensuring that $\lambda\bar{y} \ll 1$ in the first integral and that $y/\lambda \gg 1$ in the second, we can approximate the convolution for $\lambda \ll 1$ as

$$\begin{aligned} \phi{*}U(z) \sim{}& U(z) + \lambda^2U''(z)\int_0^\psi \bar{y}^2\phi(\bar{y})\mathrm{d}\bar{y} \\ &+ \frac{1}{12}\lambda^4U'''(z)\int_0^\psi \bar{y}^4\phi(\bar{y})\mathrm{d}\bar{y} + a_0\lambda^{n-1}\int_{\lambda\psi}^\infty y^{-n}G(U, z, y)\mathrm{d}y. \end{aligned} \tag{89}$$

In order to deal with the obvious problems of convergence in the first and second integrals if we extend the range to infinity and in the third if we extend it to zero, we must deal separately with the cases $3 < n < 5$ and $1 < n < 3$.

3.2.1. Case 2(a): $3 < n < 5$. In this case $\int_0^\infty \bar{y}^2\phi(\bar{y})\mathrm{d}\bar{y}$ exists, but neither $\int_0^\infty \bar{y}^4\phi(\bar{y})\mathrm{d}\bar{y}$ nor $\int_0^\infty y^{-n}G(U,z,y)\mathrm{d}y$ exist. By carefully dealing with the relevant singularities, we can show that

$$\begin{aligned}\phi * U(z) \sim\ & U(z) + \lambda^2 k_2 U''(z) + \frac{1}{12}\lambda^4 U''''(z)\int_0^\infty \left\{\bar{y}^4\phi(\bar{y}) - a_0\bar{y}^{4-n}\right\}\mathrm{d}\bar{y}\\ & + a_0\lambda^{n-1}\left[\int_1^\infty y^{-n}G(U,z,y)\mathrm{d}y + \int_0^1 \left\{y^{-n}G(U,z,y)\right.\right.\\ & \left.\left. - y^{2-n}U''(z)\right\}\mathrm{d}y\right]. \qquad (90)\end{aligned}$$

By comparing with the expansion (77) that we used in case 1, we can see that the asymptotic analysis proceeds in the same way up to $O(\lambda^2)$. The term of order λ^{n-1} is antisymmetric in z when $U = U_{\min}$, and so generates a correction to U but not to the wavespeed, and finally, the correction to the wavespeed occurs at $O(\lambda^4)$, with the U'''' term in (90) not making a contribution. In other words, the leading order corrections to U and $c_{\min}$ are given by the analysis presented in section 3.1.

3.2.2. Case 2(b): $1 < n < 3$. In this case, $\int_0^\infty y^{-n}G(U,z,y)\mathrm{d}y$ exists, but $\int_0^\infty \bar{y}^2\phi(\bar{y})\mathrm{d}\bar{y}$ does not. By again carefully dealing with the relevant singularities, we find that

$$\begin{aligned}\phi * U(z) \sim\ & U(z) + a_0\lambda^{n-1}\int_0^\infty y^{-n}G(U,z,y)\mathrm{d}y + \lambda^2 U''(z)\\ & \times\left[\int_0^1 \bar{y}^2\phi(\bar{y})\mathrm{d}\bar{y} - \frac{a_0}{(3-n)} + \int_1^\infty \left\{\bar{y}^2\phi(\bar{y}) - a_0\bar{y}^{2-n}\right\}\mathrm{d}\bar{y}\right]. \qquad (91)\end{aligned}$$

The asymptotic analysis proceeds in the same way as it did in case 1, with a correction to U, but not to $c_{\min}$, at $O(\lambda^{n-1})$. The correction to the minimum wavespeed comes at $O(\lambda^{2(n-1)})$, with the $O(\lambda^2)$ term in (91) having no effect because it is antisymmetric in z when $U = U_{\min}$.

Although we were able to find the correction terms for U and $c_{\min}$ analytically in case 1, the combination of algebraic and exponential terms in $y^{-n}G(U_{\min},z,y)$ means that this is not possible in this case. Finding simple expressions for them is however straightforward based on the analysis presented in section 3.1. We find that $U \sim U_0 + \lambda^{n-1}U_1$, with $U_0 = U_{\min}(z)$ and

$$U_1 = a_0 U_0'(z)\int_0^z \frac{\mathrm{e}^{-c_0 q}}{U_0'(q)^2}\int_{-\infty}^q \mathrm{e}^{c_0 s}U_0'(s)U_0(s)^2\int_0^\infty y^{-n}G(U_0,s,y)\mathrm{d}y\,\mathrm{d}s\,\mathrm{d}q, \qquad (92)$$

and $c \sim \frac{1}{\sqrt{2}} + \lambda^{2(n-1)}c_2$, with c_2 given by (85), but with

$$\begin{aligned}F(z) \equiv\ & -U_1^2(z) + 3U_0(z)U_1^2(z) + a_0 U_0(z)\\ & \times\left\{U_0(z)\int_0^\infty y^{-n}G(U_1,z,y)\mathrm{d}y + 2U_1(z)\int_0^\infty y^{-n}G(U_0,z,y)\mathrm{d}y\right\}. \qquad (93)\end{aligned}$$

Moreover, it is possible to find the q and s integrals in (92) analytically using symbolic algebra. However, the resulting expressions are very badly conditioned for large and small y. It is therefore more straightforward to find U_1 numerically by solving the linear boundary value problem satisfied by $\bar{U}_1 \equiv U_1/a_0$, namely

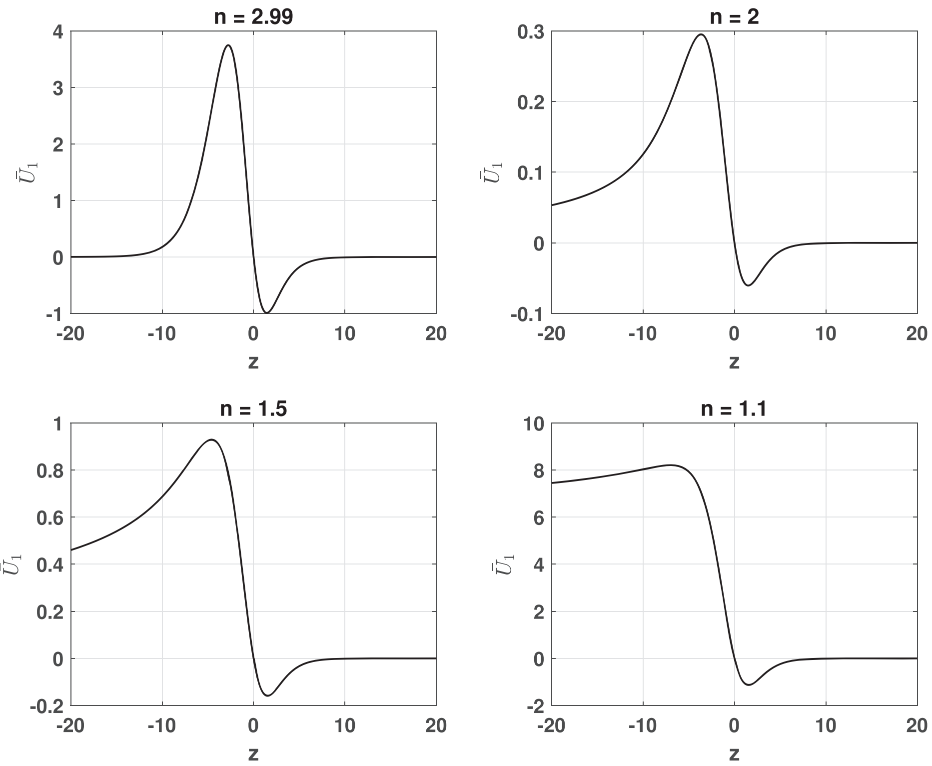

Figure 4. The scaled correction to the leading order solution, $\bar{U}_1$ for various values of n.

$$\bar{U}_1'' + c_0\bar{U}_1' + U_0(2 - 3U_0)\bar{U}_1 = U_0^2 \int_0^\infty y^{-n} G(U_0, z, y)\mathrm{d}y, \tag{94}$$

to be solved subject to

$$\bar{U}_1 \to 0 \quad \text{as } z \to \pm\infty. \tag{95}$$

We truncate (94) to a finite domain and solve using bvp5c in MATLAB. Since U_0' is a solution of the homogeneous version of (94), we can add an appropriate multiple to the numerical solution to satisfy the phase condition, $\bar{U}_1(0) = 0$. Note that it is straightforward to show from (94) that $\bar{U}_1 \sim \frac{1}{(n-1)}(-z)^{-(n-1)}$ as $z \to -\infty$, and we use this in our numerical solution to improve convergence. This also shows that the travelling wave solution approaches its equilibrium value only algebraically fast as $z \to -\infty$, and indicates how the solution breaks down as $n \to 1^+$. Some typical solutions are shown in figure 4. As we should expect, the solution approaches the same functional form as in case 1, shown in figure 3, as $n \to 3^-$. As n decreases towards unity, the rate of decay of the correction becomes slower as $z \to -\infty$.

The correction to the wavespeed is given, after evaluating the denominator of (85) analytically, by

$$c_2 = a_0^2 \bar{c}_2, \qquad \bar{c}_2(n) = 3\sqrt{2} \int_{-\infty}^{\infty} \mathrm{e}^{c_0 s} U_0'(s)\bar{F}(s)\mathrm{d}s, \tag{96}$$

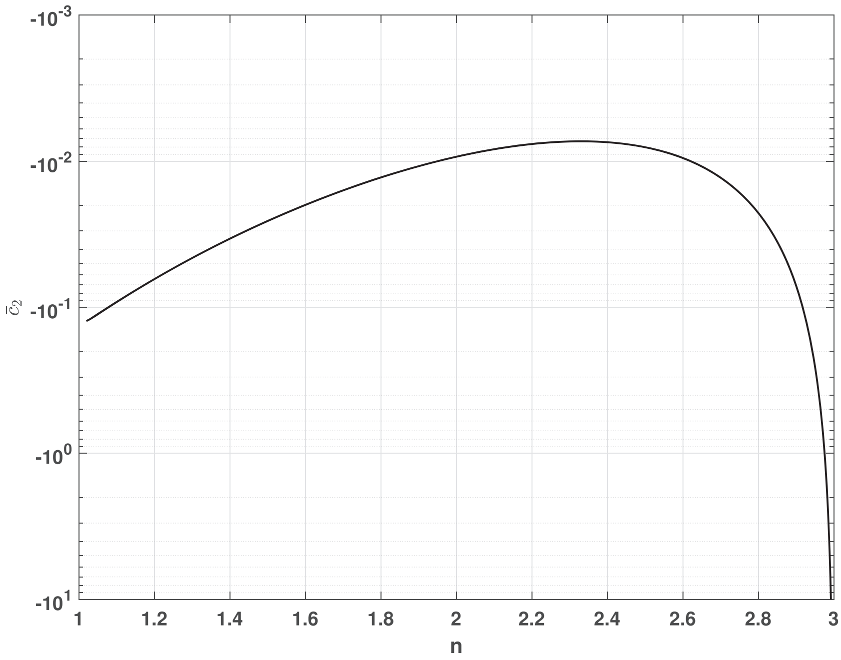

Figure 5. The scaled wavespeed, $\bar{c}_2$ as a function of n, the algebraic rate of decay of the kernel as $y \to \infty$.

with

$$\bar{F}(z) \equiv -\bar{U}_1^2(z) + 3U_0(z)\bar{U}_1^2(z) + U_0(z) \times \left\{ U_0(z)\int_0^\infty y^{-n}G(\bar{U}_1, z, y)\mathrm{d}y + 2\bar{U}_1(z)\int_0^\infty y^{-n}G(U_0, z, y)\mathrm{d}y \right\}. \quad (97)$$

Figure 5 shows the computed value of $\bar{c}_2$. Consistent with the behaviour that we found in case 1, the correction to the wavespeed is negative and, since we would expect a correction logarithmic in λ when $n = 3$, $\bar{c}_2$ appears to be singular as $n \to 3^-$. In contrast, $\bar{c}_2$ appears to be regular as $n \to 1^+$. In this limit, however, the problem becomes ill-posed, as the kernel cannot be normalised to have unit area.

4. Numerical solutions

In order to solve (13) to (15) numerically, we begin by truncating to a finite domain, $-L \leqslant z \leqslant L$, and discretise using a uniform grid of N points. We use central finite differences to evaluate the derivatives and assume a linear variation of U on each element, between the nodes. The convolution integral is evaluated using 16 point Gaussian quadrature to accurately capture the variation of the kernel across each element, collocating at each interior node. This accurate resolution of the kernel is important for convergence in extreme cases when the kernel is algebraic and n close to one. We apply the discrete version of the boundary condition $U' + cU = 0$ at $z = L$ in order to select the exponentially-decaying travelling wave solution, and also enforce $U = \frac{1}{2}$ at $z = z_0$ to fix the phase of the solution. In the solutions

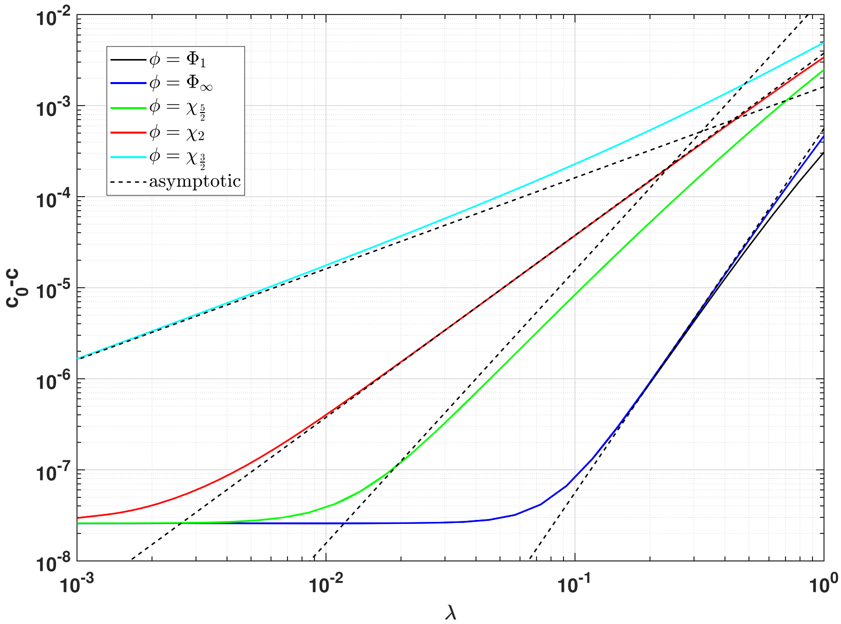

Figure 6. Comparison between the correction to the minimum wavespeed calculated numerically (solid lines) and asymptotically for $\lambda \ll 1$ (broken lines). Note that the correction is swamped by numerical error once the size of the correction falls below about 10^{-7}. For larger values of the correction, there is encouraging agreement between the numerical and asymptotic solutions.

presented below, we used $N = 24\,000$, $L = 20$ and $z_0 = 5$. At $z = -L$ we apply the boundary condition $U = 1$ for the exponential kernels $\phi = \Phi_1$ and $\phi = \Phi_\infty$. The contribution to the convolution from $z < -L$ is approximated by assuming that $U = 1$ for $z < -L$, and the integral evaluated analytically. For algebraic kernels, $\phi = \chi_n$, we use the farfield condition $U = 1 + \frac{a_0}{n-1}\left(-\frac{z-z_0}{\lambda}\right)^{-(n-1)}$. The contribution to the convolution from $z < -L$ is approximated by assuming that $U = 1 + \frac{a_0}{n-1}\left(-\frac{z-z_0}{\lambda}\right)^{-(n-1)}$ for $z < -L$, and the integral calculated using 'integral' in Matlab. The resulting set of algebraic equations was solved in Matlab using 'fsolve', with the Jacobian supplied analytically to speed up the algorithm.

Figure 6 shows the numerical and asymptotic approximations to the correction to the wavespeed as a function of λ for various kernels. In most cases there is reasonable agreement between the asymptotic and numerical values, until the size of the correction becomes comparable to the numerical error, around 10^{-7}. For $\phi = \chi_{5/2}$, although the numerically-calculated value approaches the asymptotic value as λ decreases, it has not reached good agreement before numerical error invalidates the comparison. This effect becomes more pronounced as n approaches the edge case, $n = 3$, for the algebraic kernels $\phi = \chi_n$. We also note that the corrections to both the wavespeed and the travelling wave profile become larger as the rate of decay of the kernel decreases, which seems reasonable since this models an increasing rate of intraspecies competition. In each case, the numerically-calculated correction to U is indistinguishable from the asymptotic forms shown in figure 4 for sufficiently small λ. Note that we have not included results from the top-hat kernel, since $k_2 = 1/24$, and we were unable to calculate sufficiently accurate solutions to resolve the tiny correction to the wavespeed.

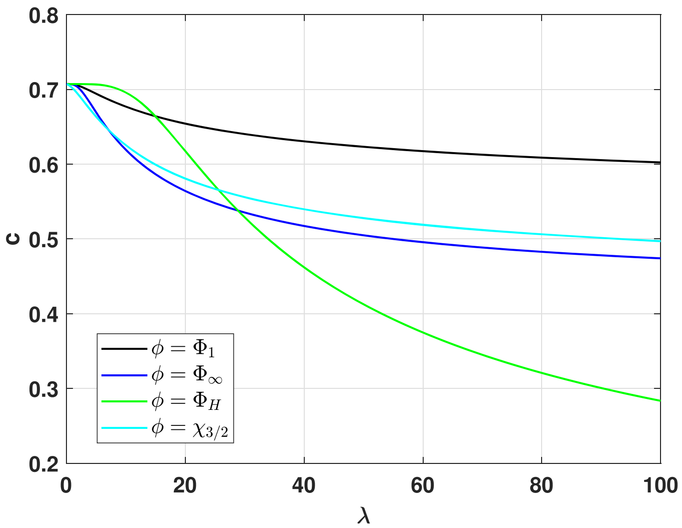

Figure 7. The minimum wavespeed as a function of λ for some of the kernels defined in the text.

Although the quantitative part of this paper has been mainly concerned with the details of PTW solutions of type E when $\lambda \ll 1$, we would also like to present some PTW solutions of type E for larger values of λ. We are currently studying the asymptotic solution for $\lambda \gg 1$ but, as we would expect from the analysis presented in [12], this is significantly more difficult to unravel than the solution for $\lambda \ll 1$, and is strongly dependent on the functional form of the kernel. Figures 7 and 8 show some results for $\phi = \Phi_1$, Φ_∞, Φ_{H} and $\chi_{3/2}$. As illustrated in figure 7, the wavespeed decreases monotonically as λ increases up to $\lambda = 100$. For large values of λ, an adaptive regridding method is needed, which will be described in part II of this series of papers. Figure 8 shows the solution when $\lambda = 100$ for these four kernels. In each case, U is maximum just behind the wavefront, and there is a decaying oscillation as $z \to -\infty$. It appears that the more slowly the amplitude of the oscillation behind the wavefront decays, the slower the solution propagates, and we will address this observation in more detail in part II. The solution for the continuous kernels, $\phi = \Phi_1$, Φ_∞ and $\chi_{3/2}$ are qualitatively similar to the equivalent solutions for the NLFKPP, as described in [12], but with some quantitative differences, which are currently under investigation. For $\phi = \Phi_{\mathrm{H}}$ ([12] did not consider discontinuous kernels), the solution has oscillations of shorter wavelength and greater amplitude than those for the three continuous kernels. The asymptotic solution for $\lambda \gg 1$ ($D \ll 1$) and $\phi = \Phi_{\mathrm{H}}$ remains to be constructed for both the quadratic and cubic NLFKPP equations.

Finally, we would also like to briefly consider the initial value problem given by (4) with localised initial conditions

$$u(x,0) = \begin{cases} \dfrac{1}{10}(1 - 4x^2) & \text{for } |x| \leqslant \dfrac{1}{2}, \\ 0 & \text{for } |x| \geqslant \dfrac{1}{2}. \end{cases}$$

This can be obtained numerically using a simple finite difference method with adaptive time stepping (see [13] for details). When the kernel and parameters are such that the steady state

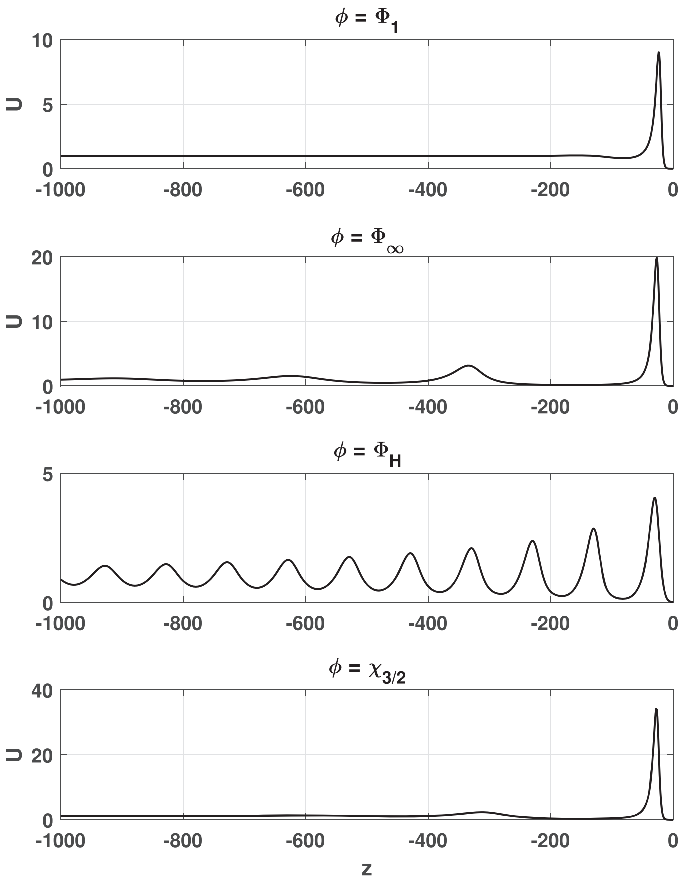

Figure 8. The travelling wave solution with minimum wavespeed when $\lambda = 100$ for some of the kernels defined in the text. Note that all solutions are computed on a domain large enough to capture the decaying oscillations for z large and negative, but has been truncated in this figure for comparison.

$u = 1$ is temporally stable we find, in every simulation we performed, that a pair of minimum speed PTW travelling waves of type E, propagating in opposite directions, is generated. However, when the steady state $u = 1$ is temporally unstable (for the kernels considered in this paper this means the top hat kernel, $\phi = \phi_{\mathrm{H}}$, with $\lambda > \lambda_0$, where $\lambda_0 \approx 18.26$, see [13] for details of the stability analysis), we find that a static, stable, periodic pattern forms behind the wavefront, with now the wavefront moving at a speed close to, but not exactly equal to, the minimum travelling wavespeed for PTWs of type E. Figure 9 shows the evolutionary solution when $\lambda = 100$. By comparing with the associated minimum speed PTW travelling wave solution shown in figure 8, it can be seen that there is little similarity in spatially propagating structure. However, figure 10 shows the position of the evolving wavefront (defined to be the largest value of x at which $u = \frac{1}{2}$), which moves slightly more slowly than the minimum speed PTW travelling wave, but is surprisingly close to this speed given the lack of detailed similarity of these two structures. A similar phenomenon occurs with the quadratic NLFKPP equation, but the agreement in evolving propagation speeds is much closer, since, in this case, this speed is generically determined locally, ahead of the wavefront. For the cubic problem that

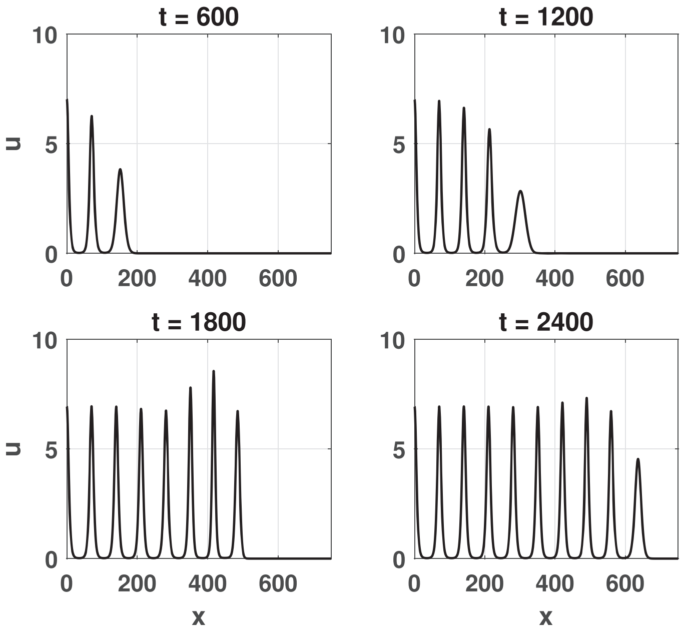

Figure 9. The development of a stationary spatial pattern from a localised initial disturbance to $u = 0$ with the top hat kernel, $\phi = \phi_{\mathrm{H}}$ and $\lambda = 100$.

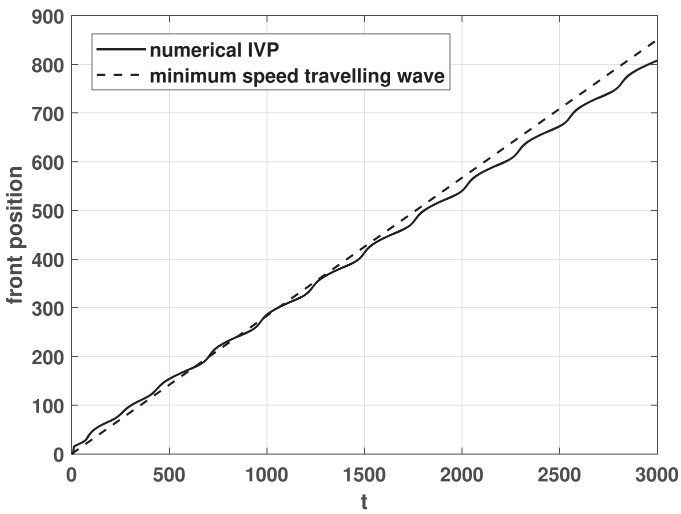

Figure 10. The position of the wavefront for the solution shown in figure 9. The dashed line shows the speed of the minimum speed travelling wave (see figure 8).

we study here, the wavespeed for PTWs is no longer determined locally, but now globally, so the agreement shown in figure 10 is not necessarily expected, and quite surprising.

5. Conclusion

In this paper we have studied the permanent form travelling wave solutions of the cubic, NLFKPP, (4). We showed that there exists a minimum wavespeed $c_{\min}(\lambda)$. We also showed that the (λ, c) parameter space contains the open region $\mathcal{A}$, defined in the introduction, where there exists a travelling wave solution with $U(z;\ c, \lambda) \sim c/z$ as $z \to \infty$, and at the closure of which there exists a unique (up to translation) travelling wave solution with $U(z;\ c, \lambda) = O(\mathrm{e}^{-cz})$ as $z \to \infty$. Numerical searches suggest that these travelling waves are the only ones available in the (λ, c) parameter space. We also constructed the asymptotic form of the exponentially-decaying permanent form travelling wave when $\lambda \ll 1$, which we found to be unique, consistent with there being a minimum wavespeed $c_{\min}(\lambda)$ such that there is a unique (up to translation) algebraically-decaying solution for each $c > c_{\min}(\lambda)$, and a unique (up to translation) exponentially-decaying solution when $c = c_{\min}(\lambda)$ for λ sufficiently small (the near local limit). We also found that the rate of decay of the kernel $\phi(y)$ as $y \to \infty$ affects the order of magnitude of the correction to the wavespeed, with $c = \frac{1}{\sqrt{2}} + O(\lambda^{2(n-1)})$ for $\phi(y) = O(y^{-n})$ as $y \to \infty$ and $1 < n \leqslant 3$ and $c = \frac{1}{\sqrt{2}} + O(\lambda^4)$ otherwise.

By numerically solving an initial value problem with localised initial conditions, we were able to observe that the travelling wave solution with minimum wavespeed emerges as the long time solution in all the cases that we studied where the kernel was such that the steady state $u = 1$ is stable. Strictly speaking, by 'minimum wavespeed' we mean that branch of exponentially-decaying travelling wave solutions that originates at $c = 1/\sqrt{2}$ when $\lambda = 0$ and can be continued numerically for $\lambda > 0$ (see figure 7). In all cases that we studied, the emerging travelling wave solution appeared to be stable. It would be interesting to perform a linear stability analysis on the travelling wave solutions to confirm this, but this is beyond the scope of the present paper.

For the top hat kernel, with λ large enough that the steady state $u = 1$ is unstable, we found that a travelling wavefront emerges, ahead of a region where a stationary pattern is created. Surprisingly, the speed of this wavefront is close to that of the minimum speed permanent form travelling wave solution, even though $u \ll 1$ in the wavefront and the wavespeed of the travelling wave solution is determined globally.

In future work, we hope to be able to construct the asymptotic solution when $\lambda \gg 1$ (equivalently, $D \ll 1$) using the methods described in [12] that were successful for the quadratic NLFKPP (this will be part II of this series of papers). The additional factor of u in the source term will affect how the solution is constructed, but, as we saw in figure 8, the qualitative nature of the solution appears to be similar.

ORCID iDs

J Billingham https://orcid.org/0000-0002-4392-5770

References

[1] Berestycki H, Nadin G, Perthame B and Ryzhik L 2009 *Nonlinearity* **22** 2813–44
[2] Billingham J and Needham D 1991 *Dyn. Stab. Syst.* **6** 33–49
[3] Li J, Chen L and Surulescu C 2020 *J. Differ. Equ.* **269** 9090–122
[4] Volpert V 2014 *Nonlocal Reaction–Diffusion Equations* (Berlin: Springer) pp 521–626
[5] Chen L, Painter K, Surulescu C and Zhigun A 2020 *Phil. Trans. R. Soc.* B **375** 1807
[6] Lorz A, Mirrahimi S and Perthame B 2011 *Commun. Partial Differ. Equ.* **36** 1071–98

[7] Lorz A, Lorenzi T, Hochberg M E, Clairambault J and Perthame B 2013 *ESAIM Math. Model. Numer. Anal.* **47** 377–99
[8] Escaff D, Fernandez-Oto C, Clerc M G and Tlidi M 2015 *Phys. Rev.* E **91** 022924
[9] Li J, Latos E and Chen L 2017 *J. Differ. Equ.* **263** 6427–55
[10] Alfaro M, Coville J, Coville G and Raoul G 2014 *Discrete Continuous Dyn. Syst.* **34** 1775–91
[11] Stegemerten F, Gurevich S V and Thiele U 2020 *Chaos* **30** 053136
[12] Billingham J 2020 *Nonlinearity* **33** 2106–42
[13] Needham D, Billingham J, Ladas N and Meyer J *J. Differ. Equ.* (submitted)
[14] Perko L 2001 *Differential Equations and Dynamical Systems* (Berlin: Springer)
[15] Hale J 1979 *Studies in Ordinary Differential Equations* (New York: Wiley)